TAO, Vol. 8, No. 4, 443-460, December 1997

Geoelectrical Surveys of Southwestern Taiwan

Chow-Son Chen[1] and Chien-Chih Chen[1]

(Manuscript received 29 July 1996, in final form 26 November 1997)

ABSTRACT

Using the Transient Electromagnetic (TEM) method, the resistivity pattern of the southwestern Taiwan was mapped and used as part of an integrated coastal environmental change study. A SIROTEM in loop configuration with square transmitting loops about 50 m on each side was used in this survey. More than 300 soundings, covering an area of about 100 km by 20 km, were collected between 1992 and 1995.

In addition to 1D ridge regression inversions, the trend surface analysis technique was used to gain a quantitative interpretation. The results were organized into both depth slice and profile maps to study 3D environmental changes.

The regional resistivity trend is found to decrease southwestwards in the Coastal Plain. In the sediments, sand is similarly found to have gradually changed to clay along the SW direction. The two trends, in fact, seem to be well correlated. Moreover, the sediment transportation directions varied systematically from NS to WE during its deposition. On the other hand, the vertical variation patterns of the resistivities also disclosed paleosea level changes. Based on the resistivity profiles, the paleo-coastal lines progressed as far as 20 km land-ward from the present location once during 16 to 6 kyr. B. P. in the northern part of the survey area; during the same period, the southern region was still covered with seawater. All of these findings are supported by drillings as discussed in this paper.

(Key words : Coastal plain, Sea level changes, TEM, Eletrostratigraphy)

1. INTRODUCTION

In the majority of environmental studies, the principal control source deep prospecting geophysical techniques employed are two-fold: seismic reflection and/or geoelectric methods. Within available geological settings, seismic reflection provides high resolution images for stratigraphic identifications (Wang *et al.*, 1991; Wang, *et al.*, 1994a; Wang, *et al.*, 1994b). On

[1]Institute of Geophysics, National Central University, Chung-Li, Taiwan, ROC

the other hand, the reason for using geoelectric methods is not to improve the resolution of seismic reflection, but rather to measure other physical properties related to additional critical exploration objectives, namely:

(1) Soil types can be differentiated by characteristic ranges of resistivity, due to clay content. The mapping of clay layers is a common objective in site assessment, because clay has a major impact on the pathways of ground water or contamination migration. (Tsai, *et al.*, 1991; Chen, 1992; Chen, 1993a; Chen, 1993b; Chen, 1995).

(2) Electric resistivity is the only physical property dependent on dissolved solids in ground water, especially saline water. Thus, for ground water explorations, no other geophysical alternative is feasible.

Within this framework, this paper examines the sediments and saline water along the southwestern coast of Taiwan by the one of the non-traditional geoelectrical methods, the Transient Electromagnetic (TEM) method. The TEM method, originally used to locate conductive objects, provides fast parametric soundings with high sensitive to conductive layers, which allows for its use in coastal environments where knowledge of the geoelectric section is required.

2. DATA ACQUISITION AND PROCESSING

The principle of the TEM method on geophysical prospecting is similar to that of radar. Interested readers can refer to the geophysical textbooks by Nabighian (1987) and Ward (1990) for detailed information. The most important characteristics of the TEM is that the survey is unlike any other geoelectric sounding. The receiver-transmitter array does not need to widen to get deeper subsurface information. This is because the depth investigation by the TEM method is mainly a function of the recorded transient time.

A typical configuration of the TEM sounding survey is that the transmitter is connected to a square single loop of wire lying on the ground. The side length of the loop is approximately equal to the desired depth of exploration. A multi-turn receiver coil, located at the center of the transmitter loop, is connected to the receiver by means of a short cable.

To delineate sediments in the Coastal Plain and its surrounding areas, a detailed TEM survey was carried out. A SIROTEM TEM (Buselli and O'Neill, 1977) with the capability of measuring the response in a delay time range of 0.049 to 160 ms was used. Measurements were made by using an in-loop geometry with a transmitter loop measuring 45 to 50 m on each side depending on site spacing. More than 300 soundings were conducted in this area (Figure 1).

To facilitate qualitative interpretation and inversion, the values of apparent resistivity were computed from the algorithm of Spies and Raiche (1980) for in loop data. All of the TEM soundings were then analyzed by one-dimensional ridge regression inversion for quantitative interpretation. A selection of the typical field data and their inverted results are shown in Figure 2. In general, soundings on the SW part of the survey area display low resistivities, while those on the northern part display high resistivities. Their geologic significance is discussed later in this paper.

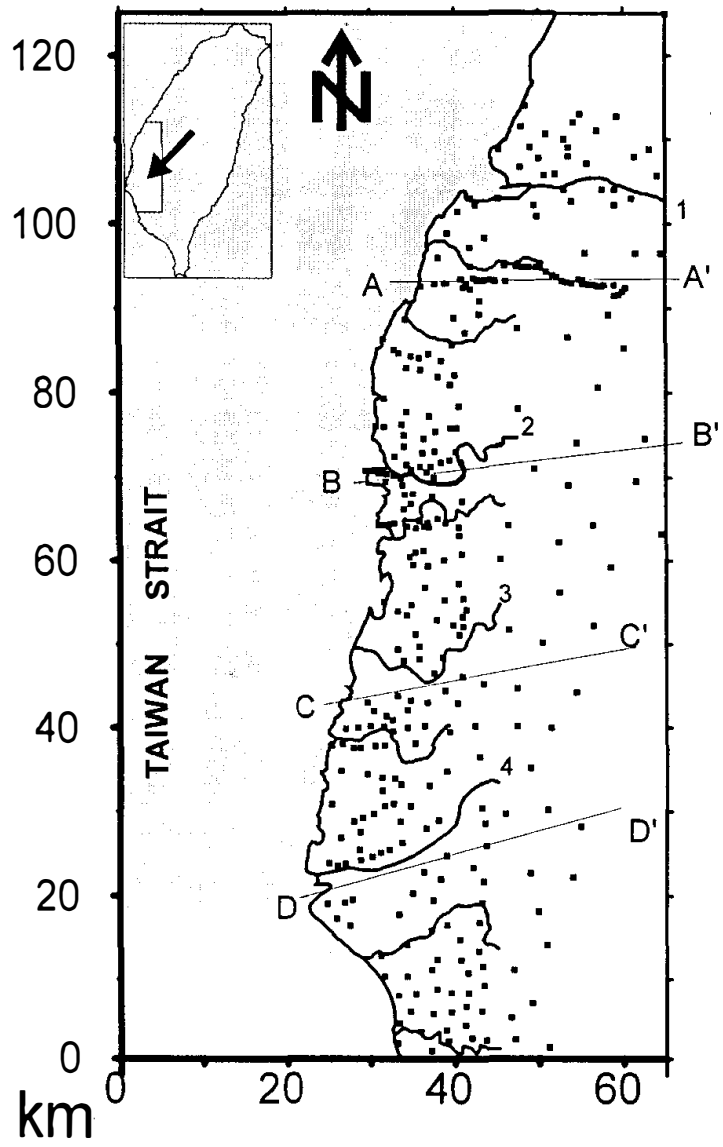

Fig. 1. Map of the studied area showing the TEM sounding locations indicated by black dots together with the 4 profiles, AA', BB', CC' and DD'. The main rivers in the survey area are: 1=Hsilo Hsi, 2=Peikang Hsi, 3= Pachang Hsi and 4= Tsengwen Hsi.

3. RESULTS AND DISCUSSION

Before presenting the TEM results, the depth of exploration in the study area was estimated first. Theoretically, the depth of TEM exploration depends on transmitter dipole moment, geoelectric structures and background noise. Therefore, this makes it not simple way to determine the precise depth of exploration. However, with the concept of the diffusion distance (Nabighian and Macnae, 1990), the depth of exploration could be approximated. The diffusion distance of transient sounding is given by:

$$d = (2 t \rho / \mu)^{1/2} \qquad (1)$$

where d: diffusion depth (m), t: time (s), ρ: resistivity (ohm-m) and μ: magnetic permeability ($4\pi \times 10^{-7}$ H/m).

Based on the TEM data along the SW coast of Taiwan, the choice of the average late time t as 10 ms (Figure 2) and the average resistivity ρ as $10^{1.2}$ = 15 ohm-m (Figure 3b) is indeed reasonable. The calculated diffusion distances are about 460 m. It should be noted that the

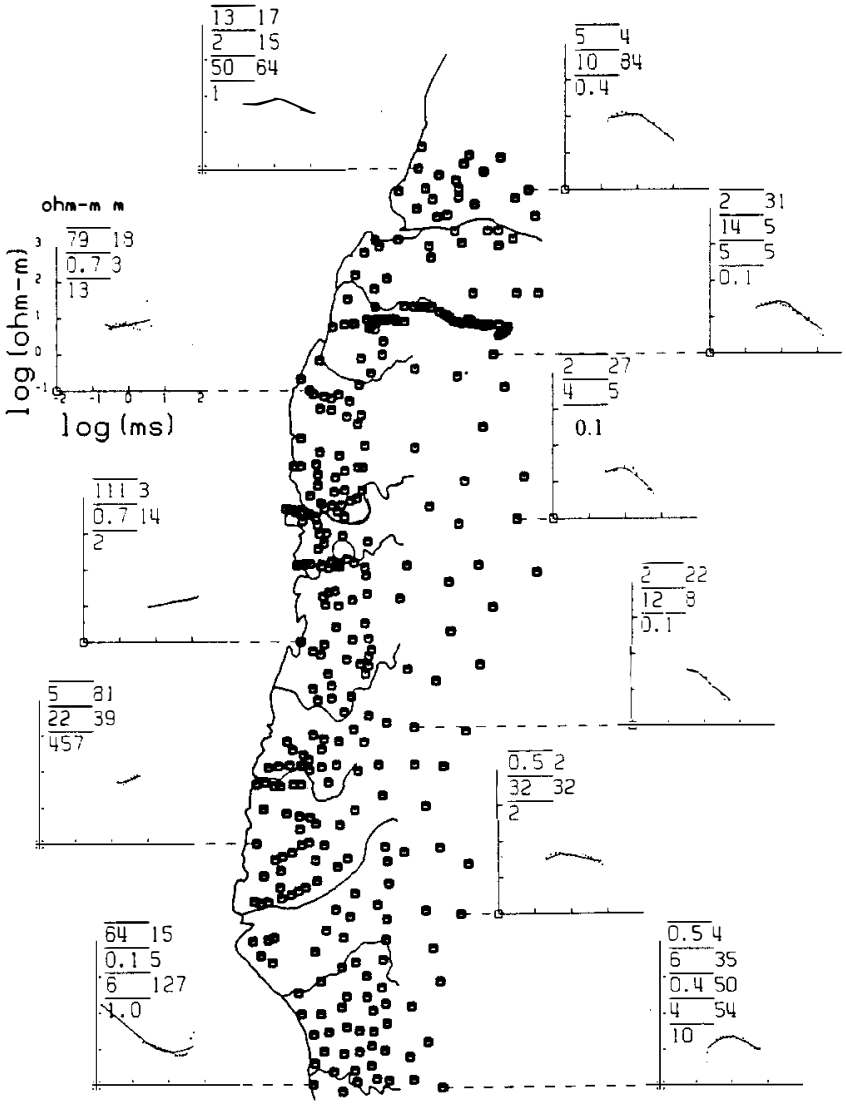

Fig. 2. A selection of the typical field data and their inverted results of the TEM soundings along the SW coast of Taiwan. Dots are field data, while the curve is the model in each inverted plot. The inverted layered earth model with resistivities in the left column and thicknesses in the right column are also shown in the upper left hand corner of the plot.

depth of exploration is generally deeper in the area farther from the coast than in that near the coast due to the higher resistivity of the former. Considering perturbation due to background noise and the need to have higher reliability, the results as to the depth within 200 m, less than one half of the diffusion depth, were focused upon here.

To assess the subsurface structures, horizontal resistivity contour maps at different depths from 10 m to 200 m were constructed. Additionally, vertical profiles were prepared. Together, these geoelectric maps provide a set of 3D structures of the SW coast of Taiwan for environmental studies.

3.1 Depth Slice Maps

Figure 3 shows 8 horizontal slices at depths 10 m, 20 m, 30 m, 50 m, 80 m, 100 m, 150 m and 200 m, respectively. The resistivities in each depth slice are displayed on a base 10 log in ohm-m. The erratic resistivity contours in each slice map may, at first, seem complicated, owing to the fact that the observed data are the outcome of two or more interacting geologic forces: one which shaped the general geologic setting and one which caused small areas to deviate from the regional pattern. This interaction is especially pronounced in coastal regions or active areas, or even both. Accordingly, the complicated resistivity pattern results, from

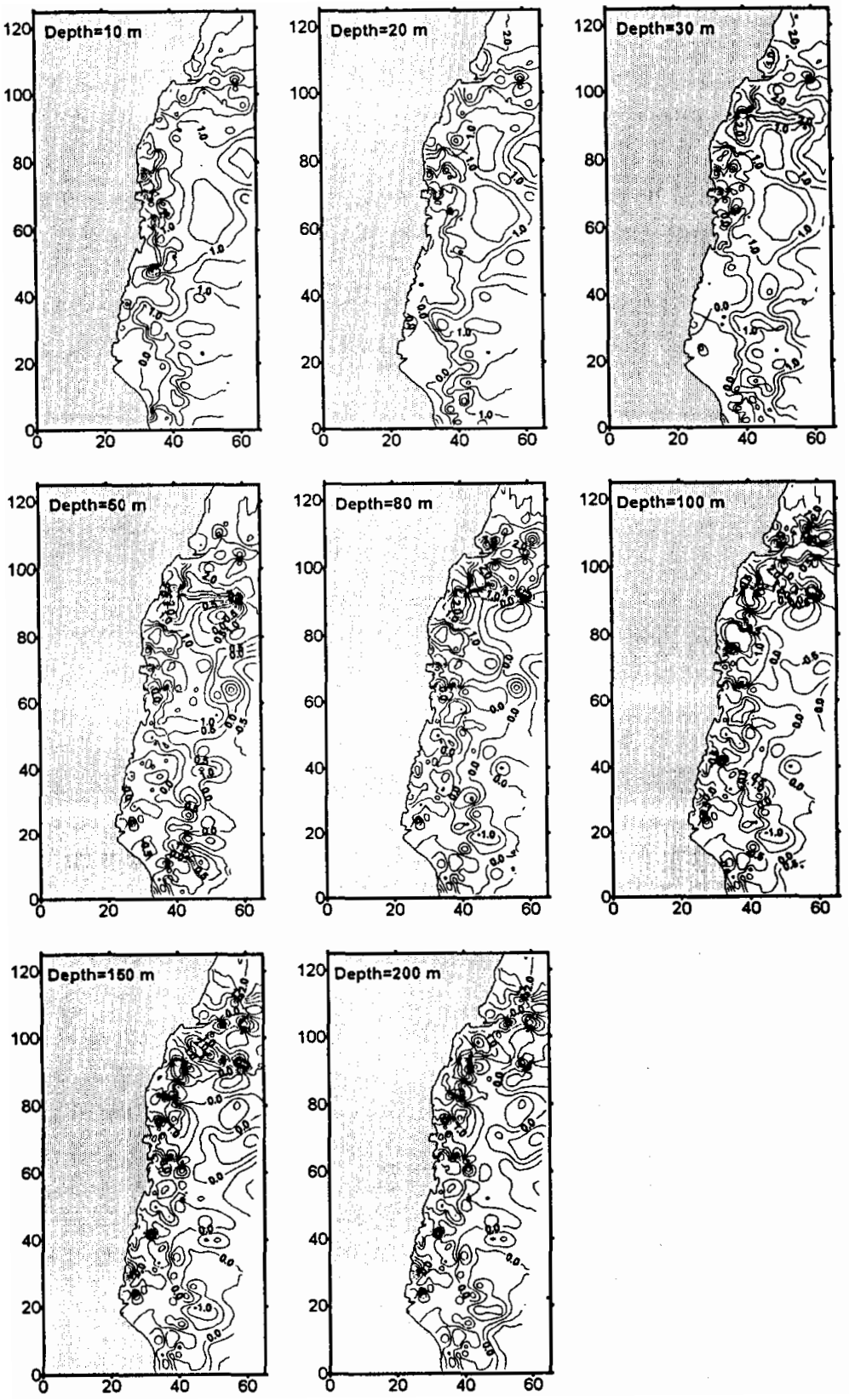

Fig. 3. Resistivity contour maps at depths 10, 20, 30, 50, 80, 100, 150 and 200 m, respectively, along the SW coast of Taiwan. The contours in each depth are displayed on a bas 10 log in ohm-m; the contour interval is 0.5.

which it is difficult to extract meaning, are to be expected.

For the sake of greater clarity, the trend surface analysis technique (Davis, 1973) was used to separate each resistivity contour map into two components, namely regional trends and local fluctuations. For example, Figure 4 shows the results of a 100-m depth map after processing by the trend surface analysis technique. In this paper, the resistivity field at the 100-m depth (Figure 4a) was used to compute, by least squares, the mathematically describable surface (first- to third- degree trend surface in this case) providing the closest fit to the resistivity field that can be obtained within a specified degree of detail. This surface is considered to be the regional resistivity variation pattern (Figure 4b), and the residual (Figure 4c) was thus determined by the difference between the resistivity field as actually mapped and the regional field. Since the residuals (Figure 4c) may have resulted from local complexities or from noise, the regional patterns (Figure 4b) are the center of focus in this study. When compared to the diagram before trend surface analysis, the regional trend reveals clear information about the possible distributions of lithofacies. The refinement of images of the geoelectric data by proper filtering is especially significant for the complicated structures frequently met in the coastal area.

In the above polynomial trend-surface analysis, a series of equations of successively higher degrees were fitted to the data. However, this raised the question of how to select the optimal degree was. The concept of "the goodness of fit" (Allen and Krumbein, 1962) was deemed helpful and was used to determine the degree of residual. Generally speaking, the goodness of fit of the TEM data s*et al*ong the SW coast of Taiwan increases with the higher degree (Figure 5). Therefore, the optimum degree for this data set is the third-degree. The third-degree of the polynomial trend surface seems to have reasonably separated the residual component from the regional component for the TEM data in the study area. All of the resistivity contours at each depth slices were filtered by the third-degree polynomial (Figure 6).

A comparison of the resistivities in the depth slices (Figure 6) makes possible the recognition of the likely lithofacies distributions and enables that the study area be subdivided. Each subdivided region may be considered to represent specific geologic conditions. At shallow depths, less than 30 m, the resistivity patterns of the study area can be divided into two regions by the contour line $10^{1.2}$ ohm-m. The northern contours, demonstrated along about the WE strike, belong to high resistivities ranging from $10^{1.2} = 15$ to $10^{1.6} = 40$ ohm-m; conversely, the southern contours, displayed along about the NS strike, belong to low resistivities of less than $10^{1.2} = 15$ ohm-m. On the bases of correlations with the lithologies of existing wells (as detailed in the next section), the high resistivity at the northern part reflects sand or gravel, whereas the low resistivity at the southern part reflects fine sand or mud. It is worth noting that the southern resistivity pattern declines to very low resistivities ($10^{-0.4} = 0.4$ ohm-m) to the SW shoreline, indicating that the sediments change from coarse grains (such as sand) to fine grains (such as clay) from east to west.

As depth increases to less than 50 m, the northern high resistivity pattern (contours greater than $10^{1.2}$ ohm-m) enlarges and extends to as far as the Peikang Hsi (River # 2). In other words, the northern half of the area is covered with sand or gravel. As depth increases to greater than 80 m, the resistivity trend seems to decrease monotonously to the south, indicating that the southern part of the survey area is mainly covered with fine sand or mud.

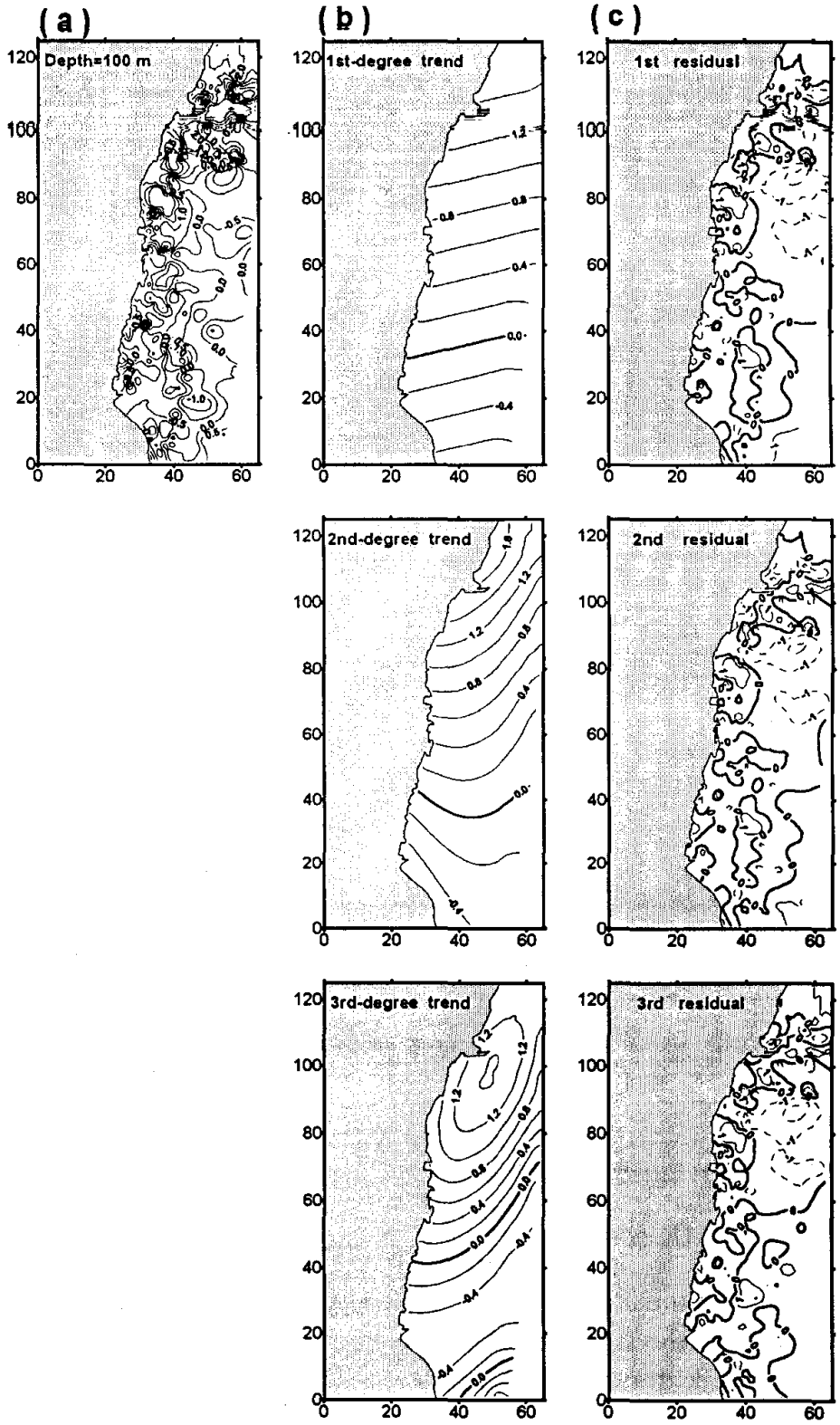

Fig. 4. (a) Resistivity contour maps at the depth of 100 m along the SW coast of Taiwan. (b) Corresponding first-, second-, and third-degree trend surface. (c) Corresponding first-, second-, and third-degree residuals. The regional trend shows a SW decreasing trend which is hardly recognized on the observed resistivity map in (a). Contours are in $\log_{10}$ (resistivity), ohm-m.

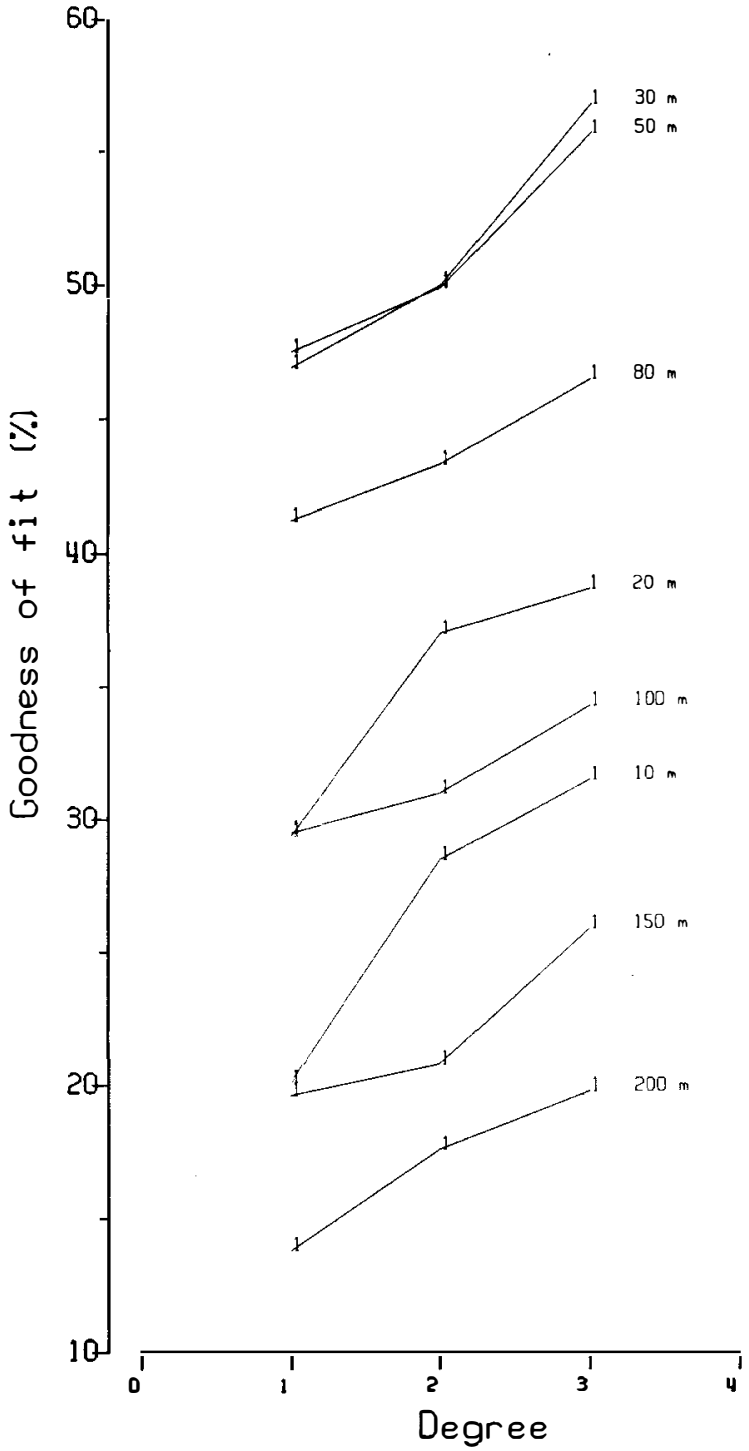

Fig. 5. Goodness of fit of the polynomial trend-surface analysis of the TEM data set along the SW of Taiwan. The number in each curve indicates depth (in meters). The optimal degree for this data set lies at the third-degree trend.

After examination of the shapes of the resistivity patterns and the ranges of resistivity values at different depths, the first conclusions concerning the area's environmental changes may be drawn. Since the sediments on the western plain of Taiwan were delivered by rivers flowing in the study area, it can be concluded that the high resistivity region corresponds to the location close to the sediment source area, while the low resistivity area represents the resting place. On the basis of the depth slices, the low resistivity location changes gradually from the west (at depth 10 m) to the south (at depth 200 m). This phenomenon strongly suggests that the direction of sediment transportation has changed in the opposite direction during the course of sedimentary history. It can be said, therefore, that the southern part of the survey area was once a final resting place of all sediments - the sea.

It is noteworthy that lithology was not the only factor controlling the resistivity patterns along the SW coast of Taiwan; on the contrary, groundwater might have also played an important role. To judge which of the two is the dominant one, additional information is required.

3.2 Wells Verification

In order to verify the above implications of the geoelectrical maps, more than 140 wells were collected (Figure 7) from many organizations, such as the Taiwan Sugar Company (TSC), the Water Conservancy Burea (WCB), the Central Geologic Survey (CGS), etc. These wells were drilled during the past 20 years; as a result, there was an absence of cores or cuttings for laboratory testing which would have been provided resistivity estimations at the present stage. Nonetheless, the lithologic columns of each well may provide conclusive evidence to dispel any ambiguity in the interpretations.

Figure 8 shows the lithofacies distributions in depth slices of the SW coast of Taiwan based on those wells. It is obvious that the deposits are mainly alluvial sediments with mud dominant in the survey area and with some aeolian sands along the coastal line. The alluvial sediments are poorly sorted in the northern half, and their grain size varies from gravel to sand and clay. The deposits in the southern half, on the other hand, are more or less well-sorted, fine-grained sand to mud.

In order to correlate the TEM results with the lithologic descriptions of wells, the regional resistivity contour maps at depths 10, 20, 30, 50, 80, 100, 150 and 200 m, respectively, are superimposed on the lithologic descriptions of wells which are displayed in the shaded maps (Figure 9). Albeit with some minor differences, the similarities between the TEM results and the lithofacies distributions are well in the northern area, clearly, higher resistivities correlate with sands or gravels. However, in the southern part, the agreement between them is not so satisfactory, especially in the southern bank of the Tsengwen Hsi (River # 4) where sands, as opposed to muds, reflect very low resistivities. The most probable reason for these discrepancies may be attributed to the large amount of groundwater. Actually, extremely low formation resistivities of less than $10^0 = 1$ ohm-m are found near the coast as a result of seawater intrusion (the average resistivity of seawater is about 0.2 ohm-m; Telford, *et al.*, 1976).

3.3 Cross-Sections

Depth slices provided the resistivity distribution in the horizontal section of common depths. In order to study the depth distribution of the resistivity, four profiles, AA', BB', CC' and DD', from north to south (Figure 1) are presented. Figure 10 illustrates the resistivity trend of each profile. The triangles indicate the sounding points. The interpreted positions of the resistivity layers and their resistivities on a base 10 log in ohm-m are contoured.

When all four cross-sections are examined (Figure 10), what becomes obvious is the westward decreasing trend of resistivity in each cross-section, suggesting that the sedimentary material was transported westward. The formation in the northeastern region (the eastern part of profile AA') has higher resistivity, indicating that the strata were formed in the stream outlet and stream sedimentary environment. In contrast, quite the reverse occurs in the south-

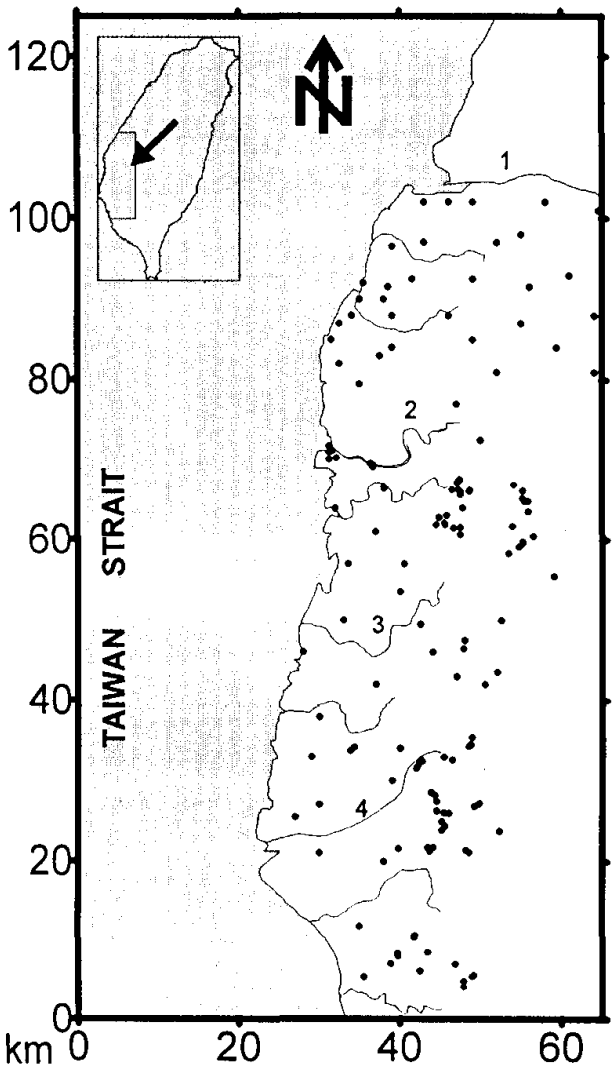

Fig. 7. Location map of wells indicated by black dots in the study area (Compiled from the CGS, the WCB and the TSC). The main rivers include: 1=Hsilo Hsi, 2= Peikang Hsi, 3=Pachang Hsi and 4=Tsengwen Hsi.

western region of the study area (the western part of profile C C'). With resistivities lower than $10^{0.0}$ = 1 ohm-m (bold contour lines in Figure 10), the region is of high salt concentration, which implies that the strata were formed in the sea or a lagoon sedimentary environment. Therefore, the isoresistivity lines of $10^{0.0}$ ohm-m separating the contact water from saline and fresh, are the boundaries of the seawater intrusion. The seawater intrusion delineated by the TEM was located as far as 20 km land-ward from the present shoreline.

In addition to the use of resistivities to recognize the possible paleo-shorelines, other stratigraphic interpretation can sometimes be inferred from the resistivity profiles. In a somewhat simplistic way, the resistivity pattern can be read as the degree of relative abundance of clay minerals and as the inverse of the 'energy' in the original depositional environment. For example, proximity to a shoreline where there was wave action represents 'high energy', with the consequent removal of clay minerals. Hence, a resistivity pattern which gradually increases in clay as the surface is approached indicates a receding shoreline and, hence, a transgressive sea (Figure 11). Conversely, an increasing in clay with depth is interpreted as a regressive sea. Accordingly, the cross-section AA' in Figure 10, for example, shows at least two episodes of transgression - one which happened at about the depth of 75 m and the other at the depth of

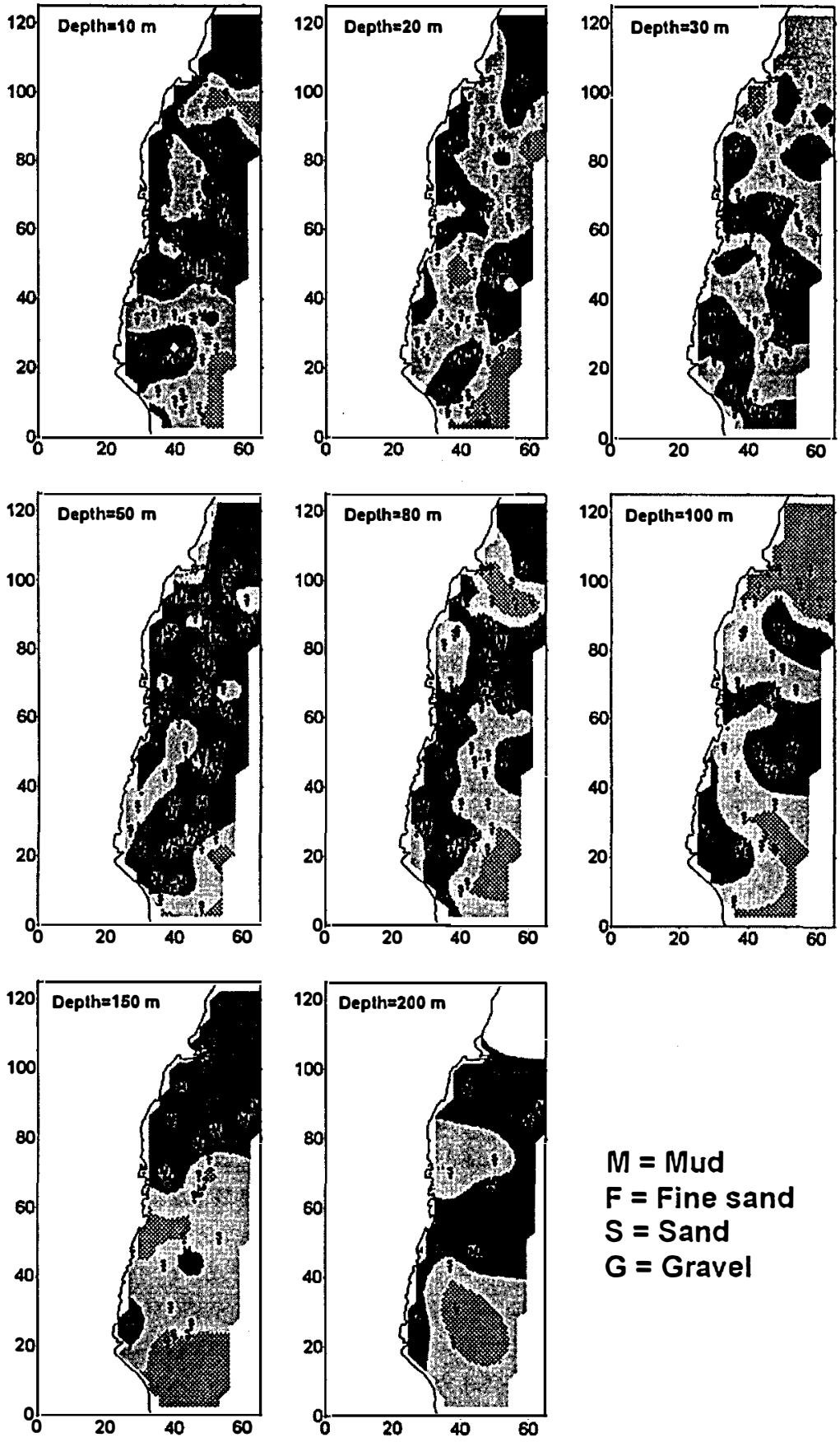

Fig. 8. Lithofacies distributions at depths 10, 20, 30, 50, 80, 100, 150 and 200 m, respectively, based on the lithologic columns of each well in Fig. 7.

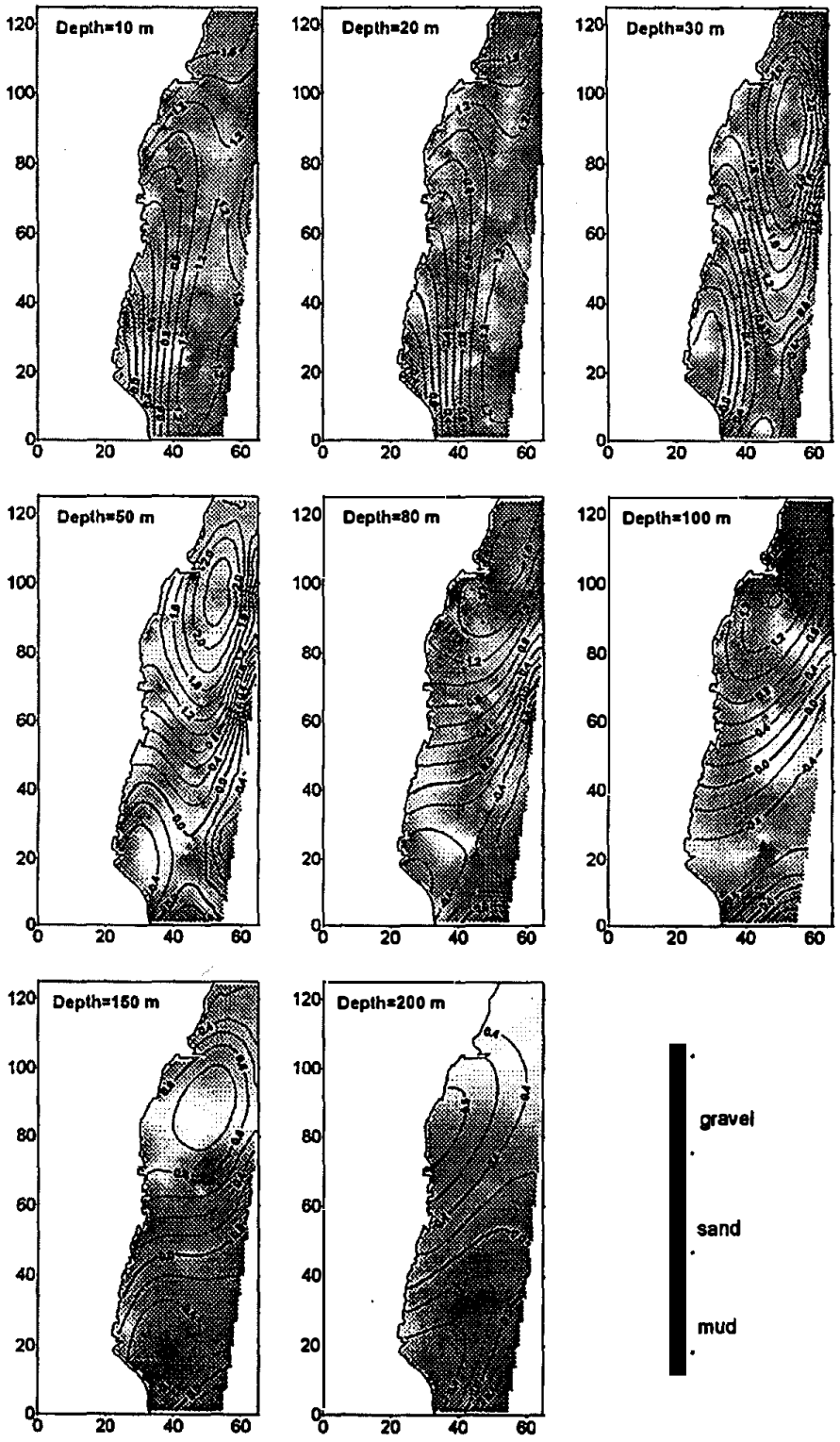

Fig. 9. Regional resistivity contour maps (in $\log_{10}$ resistivity, ohm-m) at depths 10, 20, 30, 50, 80, 100, 150 and 200 m, respectively, are superimposed on lithofacies distributions which are displayed in shaded maps. The correlation between the locations of higher resistivity contours (in the north) and the regions of gravel or sand is noteworthy.

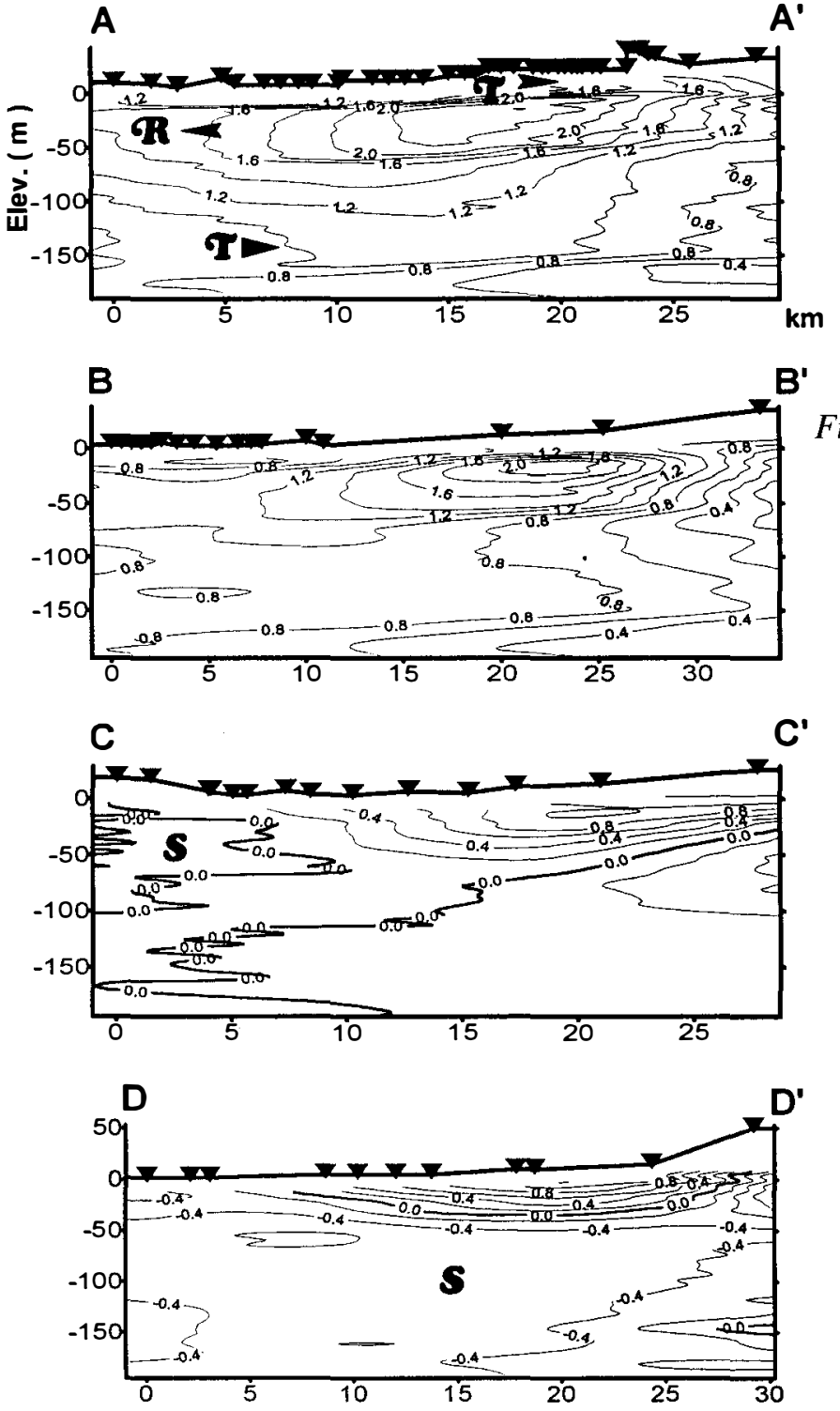

Fig. 10. Geoelectric section of profiles AA', BB', CC' and DD' in Fig. 1. The triangles on the surface topography indicate the sounding points. The interpreted positions of the layers and their $\log_{10}$(resistivity) in ohm-m are contoured. T= Transgression; R = Regression; S= Seawater intrusion.

less than 20 m. This means that the paleocoastal line as delineated in this way was located as far as 20 km land-ward from the present locations; at the same time, the southern half of the survey area was still covered with seawater. On the other hand, during the regression period, it may have been caused by the transport of many sediments which came from the eastern hills and quickly filled up the lagoons that resulted in the layer of high resistivities. Similar evidence of trangression displayed in the remaining cross-sections BB', CC' and DD' is not as obvious as that of section AA' because of groundwater interference as explained in the previous section.

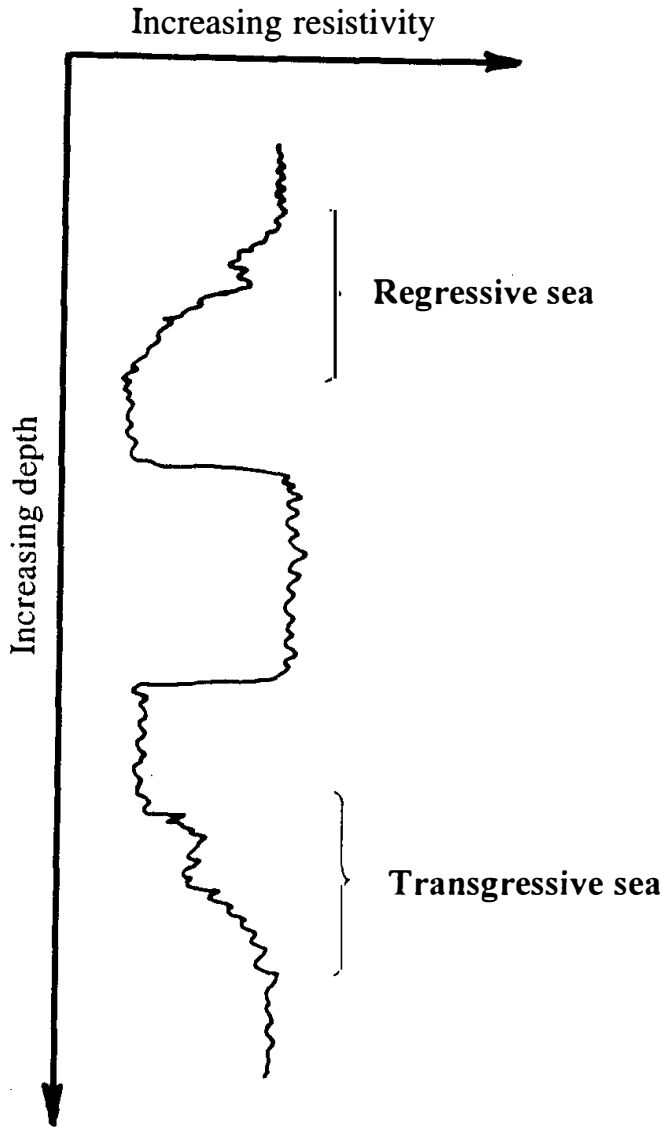

Fig. 11. Characteristic resistivity curves for transgressive and regressive seas.

It is very fortunate that, to some extent, the above arguments could be checked by the lithology of the existing wells. An intensive project of geological and water monitoring well drilling and sampling was conducted by the CGS at the same time that the AA' profile was being analyzed. There were 7 wells almost evenly distributed along this profile. C-14 dating of the sedimentary cores and core-to-core correlation of dated sections reveal lithofacies distributions in time and space (Figure 12a). For the purpose of comparison, Figure 12 illustrates both the stratigraphic columnar section (Liu, 1994) and the geoelectric section AA' on approximately the same distance scale. From the standpoint of the general trend, the tendency for the regional sediments to change from coarse grained sediments (such as gravel) to fine-grained ones (such as clay) in the western direction (Figure 12a) may be correlated with the geoelectric section from the eastern high toward the western low (Figure 12b). Meanwhile, the geoelectric profile clearly shows the presence of the twice main transgressive sea due to the decrease in resistivity as the surface is approached (Figure 12b). Radiocarbon dating of sediments at correlated depths from shallow to deep indicates that the transgressive seas happened in 6 to 16 kyr. B. P. and more than 50 kyr. B. P., respectively.

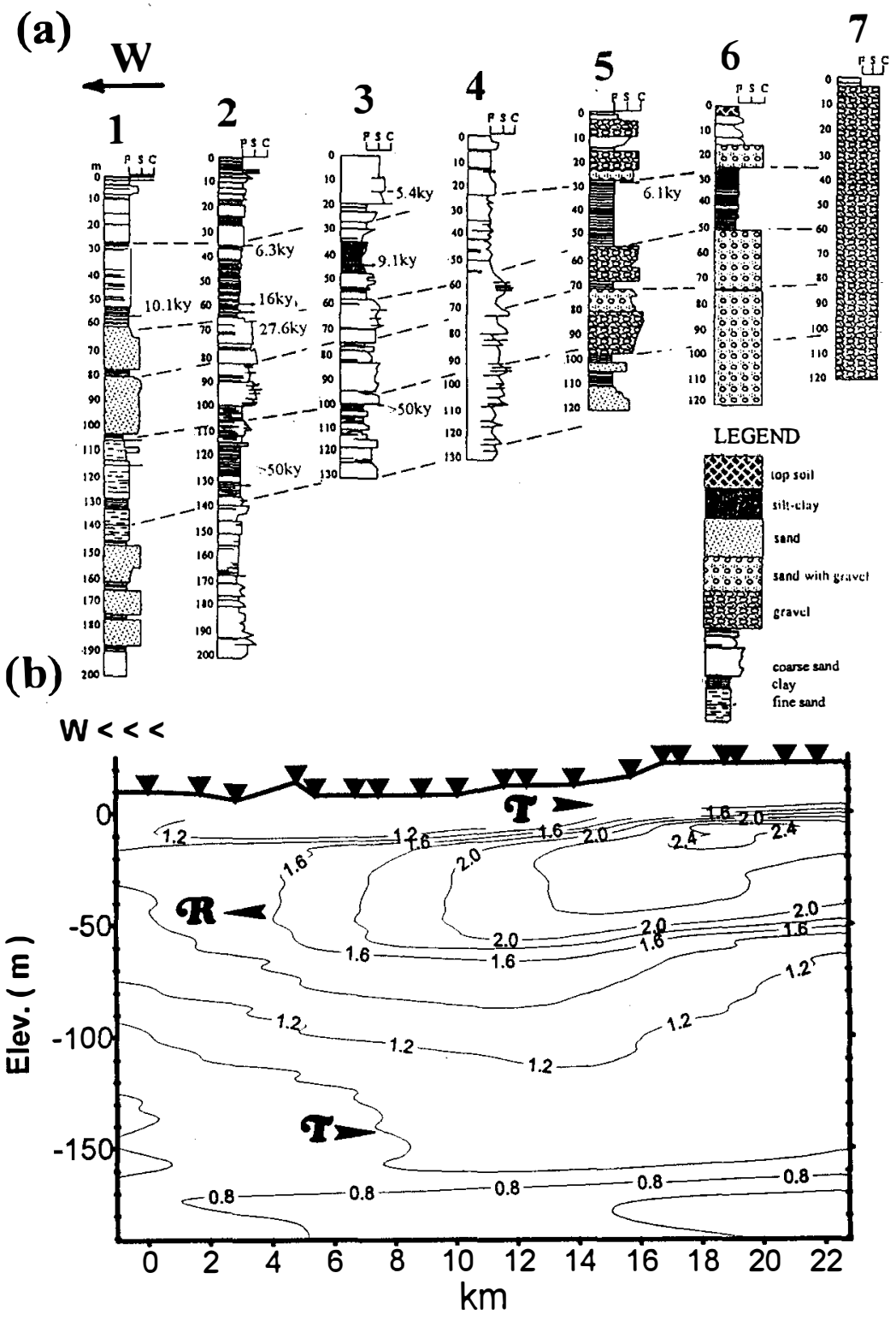

Fig. 12. (a) Geologic section of profile AA' in Fig. 1 based on 7 wells. C-14 dating of sediments are also indicated. (b) Geoelectric section of profile A A' are contoured in $\log_{10}$ (resistivity), ohm-m. The tendency for the regional sediments to change from coarse grained sediments, gravel, to fine-grained ones, clay, in the western direction clearly correlate with the geoelectric section from the eastern high toward the western low. The resistivity profile also shows the presence of twice transgressions (T) and once regression (R). Numbers on the surface indicate well locations.

4. CONCLUSIONS

Based on the results of the TEM soundings carried out in the Coastal Plain, southwestern Taiwan, this paper presents a large set of both field data and lithofacies distributions of wells to interpret the sedimentology associated with sea-level changes. The sediment of sand gradually changes to clay in the SW direction in the survey area. Moreover, the direction of the sediments appear to have changed systematically from NS to WE during the sedimentary processes. It was also discovered that the paleo-coastal lines once progressed as far as 20 km land-ward from the present location during 16 to 6 kyr. B. P. in the northern part of the survey area; at the same time, the southern region was still covered by seawater. These data on the coastal environmental changes might well be used as a local or even regional index related to further studies concerning past global changes.

Acknowledgments The authors appreciate the valuable suggestions by reviewers. This study was financially supported by the National Science Council of the Republic of China under grants NSC81-0202-N008-540, NSC83-0202-M-008-011, NSC 84-2111-M-008-045GP and NSC 85-2111-M-008-003.

REFERENCES

Allen, P., and W. C. Krumbein, 1962: Secondary trend components in the top Ashdown pebble bed: a case history, *J. Geol. Soc.*, **70**, 507-538.

Angenheister, G., Ed., 1982: Physical properties of rocks. Landolt-Bornstein, New series 1b, Springer-Verlag.

Buselli, G., and B. O'Neill, 1977: SIROTEM: a new portable instrument for multichannel transient electromagnetic measurements. *ASEG*, **8**, 82-87.

Chen, C. S., 1992: Mapping structures in the Hsinhua fault area, southwestern Taiwan by the TEM method. *J. Geol. Soc. China*, **35**, 261-273.

Chen, C. S., 1993a: Application of the CSAMT method for the gold-copper deposits in the Chinkuashih area, north Taiwan. *TAO*, **4**, 339-350.

Chen, C. S., 1993b: Urban Geophysics - TEM mapping in the Taipei Basin, Taiwan. *ASEG*, **24**, 401-406.

Chen, C. S., 1995: TEM mapping along the Longitudinal Valley in eastern Taiwan, and its tectonic implications. *TAO,* **6**, 271-283.

Davis, J. C., 1973: Statistics and data analysis in geology. John Wiley & SONS, Inc., New York, 322-337.

Liu, T. K., 1994: Evaluating groundwater flow system in an alluvial fan-delta aquifer using radiocarbon dating and tritium tracer. First conference on resources and geochemistry across the Taiwan Strait, National Central Univ., 37-41.

Nabighian, M. N., 1987: Electromagnetic methods in applied geophysics - applications. SEG, 427-520.

Nabighian, M. N., and J. C. Macnae, 1990: Time domain electromagnetic prospecting methods: geotechnical and environmental geophysics. SEG, 427-479.

Spies, B. R., and A. P. Raiche,1980: Calculation of apparent conductivity for the transient electromagnetic (Coincident loop) method using an HP-67 calculator. *Geophysics*, **45**, 1197-1200.

Telford, W. M., L. P. Geldart, R. E. Sheriff, and D. A. Keys, 1976: Applied Geophys. Cambridge Univ. Press, 770pp.

Tsai, L. L., C. S. Chen, and L. C. Sun, 1991: Acid mine drainage in the Chinkuashih-Shuinantung area. *TAO,* **2**, 297-316.

Wang, C. Y., C. H. Hsieh, D. T. Tsai, and L. W. Hsu, 1991: Experience with shallow reflection seismics as applied to the shallow structure study. *Proc. Geol. Soc. China,* **34**, 111-130.

Wang C. Y., W. C. Hsiao, and C. T. Sun, 1994: Reflection seismic stratigraphy in the Taipei Basin (1) - northeastern Taipei Basin. *J. Geol. Soc. China,* **37**, 1-28.

Wang C. Y., G. P. Chen, and D. T. Jong, 1994: The detection of the active faults on Taiwan using shallow reflection seismics. *TAO,* **5**, 120-136.

Ward, S. H., 1990: Geotechnical and environmental geophysics - vol. 2. SEG, 1-40.

Wu, D. C., Y. G. Chen, and C. G. Liu,1992: The study of the depositional history of Tainan tableland and its neo-structures. Ti-Chih, 12(2), 167-184.